Sol-gel synthesis of Se and Te containing TiO_2 nanocomposites with photocatalytic and antibacterial properties

A. BACHVAROVA-NEDELCHEVA[a,*], R. IORDANOVA[a], A. STOYANOVA[b], N. GEORGIEVA[c], TS. ANGELOVA[c]
[a]*Institute of General and Inorganic Chemistry, Bulgarian Academy of Sciences, "Acad. G. Bonchev" str., bld. 11, 1113 Sofia, Bulgaria*
[b]*Medical University, "Kl. Ohridski", str. 1, 5800 Pleven, Bulgaria*
[c]*Department of Biotechnology, University of Chemical Technology and Metallurgy, 8 Kl. Ohridski, 1756, Sofia, Bulgaria*

Two gel compositions containing 20 and 25 mol % SeO_2 ($80TiO_2.20SeO_2$ and $50TiO_2.25TeO_2.25SeO_2$) were selected for detailed investigations. The crystallization tendency in the temperature range 200 – 400°C was investigated. According to XRD analysis selenium nanoparticles dispersed in an amorphous matrix were found up to 300°C. The microprobe analysis proved presence of selenium at 400°C. The photocatalytic tests showed that the binary sample ($80TiO_2.20SeO_2$) possesses photocatalytic activity toward Malachite green organic dye. Both compositions exhibited good antimicrobial activity against *E. coli* K12.

(Received November 2, 2015; accepted February 10, 2016)

Keywords: Sol-gel, Selenium, Composite materials, Photocatalysis, Antibacterial properties

1. Introduction

The titania and TiO_2 based compounds are subjects of special interest and they are intensively studied mainly due to their good photocatalytic and antibacterial properties [1-4]. It is well known that as a wide band gap semiconductor, TiO_2 is excited only by UV-light. This disadvantage limits its utilization under solar energy. Moreover, due to the short charge separation distances within the semiconductor particle, e^-/h^+ recombination speed is too fast resulting in a decrease in the quantum yield of the process. On the other hand, a good photocatalyst depends strongly on e^-/h^+ pair separation and optical properties. That is why in the recent years the scientific research is focused on extending the optical absorption of TiO_2 to the visible region of the spectrum. Various strategies have been pursued to modify TiO_2 such as metal, non-metal ion doping, surface modification, etc. [5, 6]. However, there is a considerable controversy in the results obtained for the photocatalytic activity. Some investigators reported that the doping of TiO_2 enhances its photocatalytic activity while other groups found that it is detrimental. Obviously, the selection of a second component is very crucial in determining the overall photocatalytic activities.

It is known that selenium possesses unusual photo-optical and semiconducting physical properties and has industrial applications in devices such as photocopiers and microelectronic circuits. On the other hand, selenium is intensively examined mainly due to its basic importance for the organism. The paradox of selenium (Se) is that it is both essential and toxic. In the past decade, selenium received a great attention and has been studied for various medical applications and as a potential material for orthopaedic implants [7]. There are also a few data indicating the ability of selenium compounds to inhibit the growth of bacteria and the formation of bacterial biofilms [7]. For example, it was found that selenium nanoparticles inhibited the growth of *S. aureus*, *E. coli* and *C. albicans* [8, 9]. Recently, only one paper reported on the antioxidant and antimicrobial activity of tellurium dioxide [10]. Up to now, a few papers are devoted to the chemically derived TiO_2/SeO_2 nanocomposites, in which SeO_2 is used as a dopant in different concentrations (from 0.047 g to 10 g) in order to improve the TiO_2 photocatalytic properties [11-13]. It was also established that the addition of TeO_2 (about 8 %) could improve the photocatalytic properties of TiO_2 both in the UV and visible region [12].

The sol-gel method has been selected for preparation because it allows excellent control of product purity and composition due to the used pure precursors. It also allows overcoming the problems with the high volatilization and sublimation of SeO_2 at atmospheric pressure above 315°C as well as the decomposition of TeO_2 at temperature above 1000°C. All above mentioned and especially the fact that

there is no detailed information for the sol-gel synthesis of Se containing composite powders motivates our study. Moreover, the problems concerning the influence of selenium and tellurium on the photocatalytic and antibacterial properties are still unclear.

The aim of present study is to synthesize selenium and tellurium containing amorphous and nanocrystalline powders as well as to verify their photocatalytic and antibacterial properties. Two compositions $80TiO_2.20SeO_2$ (sample TS) and $50TiO_2.25TeO_2.25SeO_2$ (sample TTS) were selected and they were subjected for detailed investigations.

2. Experimental

2.1 Samples preparation

The main steps for the sol-gel synthesis of the selected compositions are described below. A combination of Te (VI) acid (Aldrich) along with Ti butoxide (Fluka AG), H_2SeO_3 (Merck) precursors dissolved in ethylene glycol ($C_2H_6O_2$) (99% Aldrich) were used. Telluric acid (H_6TeO_6) is selected to overcome the problem with high hydrolysis rate of tellurium (VI) alkoxide [14, 15]. All precursors dissolved in ethylene glycol were homogenized and stirred for 10-15 min and subsequently mixed and again homogenized with magnetic stirrer for 2-3 minutes. Thus, transparent gels were obtained. The aging of the gels was performed in air for several days in order to allow further hydrolysis. The as prepared gels were subjected to the stepwise heating from 200 to 400°C for one hour exposure time in air. The heat treatment was limited to 400°C bearing in mind the SeO_2 peculiarities described already above.

2.2 Samples characterization

Powder XRD patterns were registered at room temperature with a Bruker D8 Advance diffractometer using Cu-Kα radiation. The data were obtained in the range 10 to 80° 2θ with a step 0.02 and scanning time of 0.02 sec. It has to be noted that the XRD patterns obtained below 200°C are complicated due to the presence of organics. The average crystallite size of the powders was calculated using Sherrer's equation. The morphology of the samples was examined by scanning electron microscopy using a JEOL JSM 6390 electron microscope (Japan), equipped with ultrahigh resolution scanning system (ASID-3D). The accelerating voltage was 20kV, I~65 μA. The optical absorption spectra of the powdered samples in the wavelength range 200–1000 nm were investigated by an UV–VIS Spectrophotometer "Evolution 300" equipped with an integrating sphere and magnesium oxide reflectance standard used as a baseline.

2.3 Photocatalytic activity experiments

The photocatalytic activities of the synthesized powders were assessed by the degradation of the organic dye Malachite Green (MG), as a model pollutant. In a typical procedure 100 mg of the investigated sample was added to 150 ml dye solution (5 ppm) to form a suspension. Prior to irradiation, the suspensions were sonicated for 10 min, and then stirred in the dark for 30 min to ensure the establishment of adsorption/desorption equilibrium. The UV-irradiation was carried out using a black light blue lamp (Sylvania BLB 50 Hz 8W T5). Aliquot samples of the mixture (3 mL) were withdrawn before and at different time intervals during the irradiation and centrifuged in order to remove the solid particles. The change in the dye concentration in each aliquot was determined by measuring the absorbance value at 620 nm using Jenway 6505 UV-Vis spectrophotometer.

The sol-gel derived TiO_2 was used as a reference profile at the comparison of the optical and potocatalytic properties of the obtained powders.

2.4 Antibacterial activity testing

The antibacterial effect of obtained materials was tested against facultative anaerobic gram-negative *Escherichia coli* K12. The strains were obtained from the culture collection of Bulgarian National Bank of Industrial Microorganisms and Cell Cultures and were cultured on Luria-Bertani (LB) agar plates for 18 hours at 37°C before use. A single colony of *E. coli* K 12 was used for inoculating the liquid LB medium in order to maintain initial bacterial concentration 10^3 CFU/ml. The test for antibacterial activity of synthesized materials against *E.* coli K12 was performed using an assay based on the reduction of viable bacterial cells after exposure to the materials. Bacterial growth-inhibiting effect of materials was investigated by studying the ability of cultures to survive after exposure to these materials. For this aim to flasks containing 50 ml saline solution, 100 μl strain suspension and 10 mg of each material were added. Samples containing only bacterial cells without materials were used as controls. The incubation process was performed on a rotary shaker (220 rpm) at 37°C for 24 h. After that, 100 μl of each samples were dropped on LB agar surface. The plates were incubated 24 hours at 37°C followed by counting the number of colonies on the plate. To evaluate an antibacterial effect of investigated materials, the percentage of cell reduction was calculated as described in [16] between the control sample and the test sample.

Cell reduction (%) = (1- Test sample (CFU/ml)/Control (CFU/ml)) x 100.

3. Results and discussion

3.1 Phase characterization of the composites

3.1.1 XRD analysis and SEM

According to the XRD results, in the temperature range 200-300°C the samples are predominantly amorphous (Fig. 1). Elementary Se (JCPDS 65-1876) appeared only in the ternary sample TTS ($50TiO_2.25TeO_2.25SeO_2$) at 250 and 300°C while at 400°C TiO_2 (anatase) and elementary tellurium were detected. In contrast to the ternary sample, in the binary composition TS ($80TiO_2.20SeO_2$) small peaks of anatase were identified at 300°C and they became more pronounced at 400°C (Fig. 1). Bearing in mind these data it must be concluded that in the temperature range 200-400°C the obtained samples could be regarded as composite materials consisting of amorphous part and crystalline phases. The average particle size of elementary selenium (calculated using Sherrer's equation) in the ternary composition is about 36 nm at 250°C while the average crystallite size of TiO_2 (anatase) in both samples heat treated at 400°C is in the range 8 - 12 nm. For comparison Zhang et al. obtained SeO_2/TiO_2 nanocomposites by water bathing and calcining with average particle size about 10 nm [17]. On the other hand, our results concerning the phase transformations differ from those obtained by other authors. Recently, Štengl et al. [12] obtained Se and Te doped TiO_2 by homogeneous hydrolysis of Ti oxo-sulfate with urea in aqueous solution in the presence of Se and Te and they established that anatase crystallized even at 200°C. Probably, the applied method of synthesis influences on the phase transformations in the compositions during the heating.

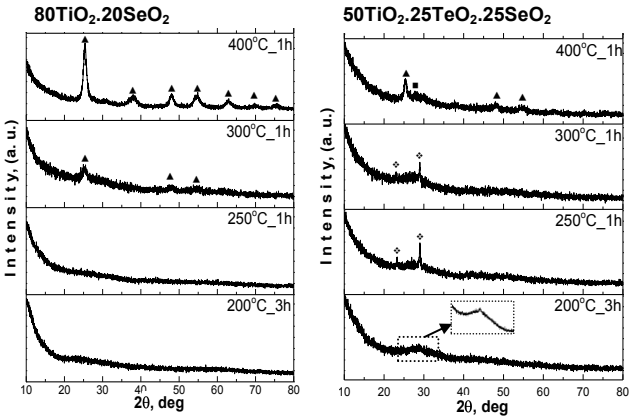

Fig. 1. XRD patterns of samples TS and TTS in the temperature range 200-400°C: (❖) Se, (■) Te, (▲) TiO_2-anatase

Both samples $80TiO_2.20SeO_2$ and $50TiO_2.25TeO_2.25SeO_2$ heat treated at 400°C were subjected for SEM investigations in order to observe the samples morphology as well as to verify the existence of selenium (Fig. 2a, b). In both samples, small pieces as a result from the crashing of the monolithic gels during the drying process are observed with average size about 50-150 μm. As it is seen small bright spots are distinguished in some areas on the sample surface. The microprobe analysis showed that selenium is segregated in these parts which mean that it is not fully evaporated even at 400°C. These results are in good accordance with the obtained XRD data where elementary selenium was detected at 300°C.

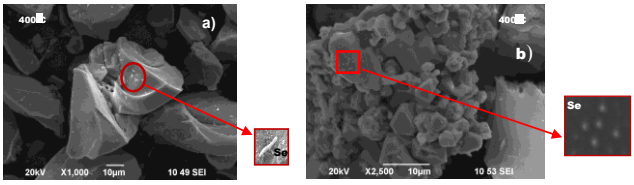

Fig. 2. SEM images of samples: a) $80TiO_2.20SeO_2$ (TS) and b) $50TiO_2.25TeO_2.25SeO_2$ (TTS) heat treated at 400°C

3.1.2 UV-Vis spectroscopy

The UV-Vis spectroscopy is used to verify the influence of Se and Te on the optical properties of TiO_2. Figure 3a, b shows the UV-Vis spectra of the gels as well as of the heated at 200 and 400°C samples (TS and TTS) compared to the spectra of pure Ti butoxide gel (Fig. 3c). As it is seen from the figure in the UV-Vis spectra of all gels two bands are distinguished centered at about 260 and 350 nm. It is known that the absorption region below 400 nm can be ascribed to the TiO_2 particles [17]. After heating at 200°C the UV-Vis spectra are changed (Fig. 3b) and a red shifting of the absorption edge in comparison to the corresponding unheated samples is observed. Despite the fact that in the binary sample elementary Se was not found by XRD, both samples (TS and TTS) exhibit a steep increased absorption above 400 nm due to the reduction processes in comparison to the spectra of pure Ti butoxide. But in the ternary sample a more pronounced long – tail visible light absorption was registered. At 200°C both samples were red coloured which is an indication for the presence of selenium. According to Nguyen et al. [18] such red shifting toward a longer wavelength observed for the Se mixed TiO_2 powder compared to pure TiO_2 is due to the heterojunction between the core TiO_2 particles and the Se particles. Moreover, some authors claimed that the red amorphous selenium does not have a sharp absorption edge but it exhibits an intensive absorption in the range 580 – 650 nm [19]. Thus, the increased visible light absorption in our samples could be related to the presence of Se. Following the Štengl et al. [12] investigations, we assume that the tellurium also contributes to this absorption. At 400°C the samples were not so intensive coloured probably because of the partial sublimation of SeO_2 at ~ 315-317°C. On the other hand, the shifting of

the absorption edge toward visible-light region was also observed in C - modified TiO_2 compositions [20-23]. It was established that the absorption increases with increasing of carbon content, which indicates that the carbon dopant is responsible for this strong visible light response [23]. The origin of absorption bands in the visible spectral range for the carbon doped TiO_2 specimens remains a hot topic of discussion. Some studies revealed that intrinsic defects, including those defects associated with oxygen vacancies, contributed to the absorption of light in the visible spectral region [24]. Therefore, we may conclude that the absorption in the obtained by us UV-Vis spectra (200, 400°C) was determined by the simultaneous presence of Se, Te and C. It has to be noticed that at these temperatures it is difficult to determine the absorption edge values due to the increasing of the background absorption from 400 to 800 nm.

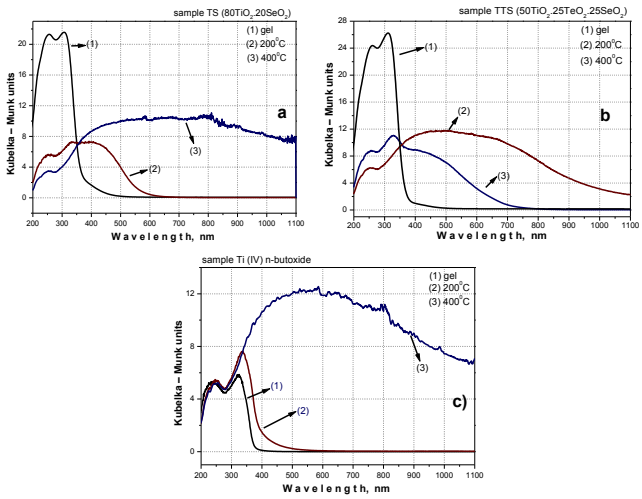

Fig. 3. UV-Vis spectra of the investigated samples: (a) $80TiO_2.20SeO_2$ (TS), (b) $50TiO_2.25TeO_2.25SeO_2$ (TTS) and (c) Ti butoxide

3.2 Photocatalytic activity

Photocatalytic decoloration of the heat treated at 200 and 400°C samples (denoted as TS-200, TS-400 and TTS-200 in Fig. 4) compared to those of TiO_2 (anatase) obtained from pure Ti butoxide by sol-gel method was tested against Malachite green organic dye under UV irradiation (Fig. 4). As it is seen from the figure, the anatase possesses photocatalytic activity and it showed decoloration efficiency about 52.6 % for 120 minutes exposure to UV light. For the same illumination period the decoloration of the binary samples heat treated at 200 and 400°C (TS-200 and TS-400) was 42 and 49 % respectively, while the ternary composition (TTS) did not exhibit any photocatalytic activity.

The photocatalytic efficiency of sample $80TiO_2.20SeO_2$ (TS-400) is comparable to those of TiO_2 (anatase) obtained by sol-gel method. The comparison of both samples (TS and TTS) shows that the simultaneous addition of TeO_2 and SeO_2 to TiO_2 did not improve the photocatalytic efficiency of the composite. Bearing in mind the above discussed UV-Vis results (Fig. 3) and the fact that carbon is present in the samples heated at 200 and 400°C, we may conclude that this is the another reason for the unsatisfied photocatalytic activity. All these preliminary results showed that the problems concerning the influence of the second component (SeO_2, TeO_2) added to TiO_2 on its photocatalytic properties is very disputable. More experiments must be performed in this direction in order to elucidate that problem. For comparison, Zhang et al. [11] found that the addition of 0.047 g selenium improved the photocatalytic efficiency of SeO_2/TiO_2 nanocomposites against methylene blue, methyl orange and rhodamine B.

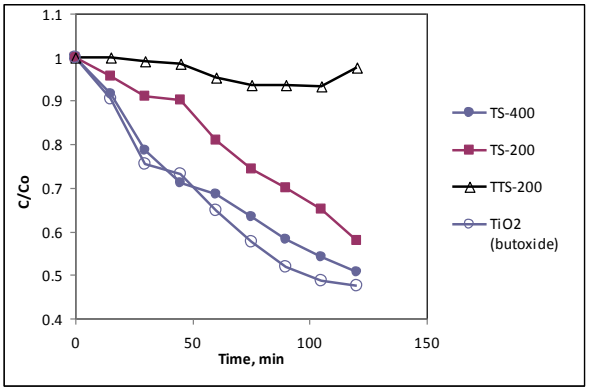

Fig. 4. Photocatalytic activity of samples TS and TTS against MG under UV irradiation.

3.3 Antibacterial test

The antibacterial properties of samples TS and TTS heat treated at 200 and 400°C were tested against *E. coli* K12. Bacterial growth was totally suppressed by $50TiO_2.25TeO_2.25SeO_2$ (sample TTS - 200) powder (Table 1). Both samples TTS - 400 and TS - 400 caused approximately 95.9 % and 86 % reduction, respectively of cells growth. The binary sample heated at 200°C (sample TS - 200) showed any inhibition of *E. coli* K12 viability. Thus, the observed antibacterial activity of our powders can be attributed to the synergetic effect of anatase, TeO_2 and elementary tellurium. On the other hand, Dědkova et al. [25] found that the presence of amorphous state in the Ce doped TiO_2 materials is one of the reason for their good antibacterial activity. Thus, it could be concluded that the amorphous state also contributes to the good antibacterial properties of the obtained composite powders.

Table 1. Antibacterial test results of E. coli K12 after 24 h cultivation

Sample	CFU/ml	Reduction of cells [%]
Control *E. coli* K12	$1x10^5$	-
$50TiO_2.25TeO_2.25SeO_2$ (sample TTS – 200)	0	100
$50TiO_2.25TeO_2.25SeO_2$ (sample TTS – 400)	$0.041x10^5$	95.9
$80TiO_2.20SeO_2$ (sample TS – 200)	$1x10^5$	0
$80TiO_2.20SeO_2$ (sample TS – 400)	$0.14x10^5$	86

4. Conclusions

By sol-gel are synthesized nanocomposites containing amorphous part and crystalline phases (anatase, Se, Te). The sol-gel derived TiO_2 obtained from pure Ti butoxide and sample $80TiO_2.20SeO_2$ heated at 400°C exhibits comparable photocatalytic activity toward MG. The obtained nanocomposite powders ($80TiO_2.20SeO_2$ and $50TiO_2.25TeO_2.25SeO_2$) possess antibacterial activity against *E. coli* K12 and they could be used as antibacterial agents.

References

[1] O. Carp, C. Z. Huisman, A. Reller, Progress in Solid State Chemistry, **32**, 33 (2004).
[2] A. Fujishima, T. Rao, D. Tryk, J. Photochem. Photobiol. C: Photochem. Rev., **1**, 1 (2000).
[3] X. Chen, S. Mao, Chem. Rev., **107**, 2891 (2007).
[4] C. Srinivasan, N. Somasundaram, Curr. Sci., **85**, 14318 (2003).
[5] A. Zaleska, Recent patents on engineering, **2**, 157 (2008).
[6] F. Han, V. S. R. Kambala, M. Srinivasan, D. Rajarathnam, R. Naidu, Appl. Catal. A Gen., **359**, 25 (2009).
[7] Q. Wang, T. J. Webster, Int. J. Nanomed., **8**, 407 (2013).
[8] E. Kheradmand, F. Rafii, Mohammad H. Yazdi, A. Akhavan Sepahi, A. Reza Shahverdi and M. Reza Oveisi, DARU J. Pharmaceutical Sci., **22**, 48 (2014).
[9] P. Verma, World J. Pharm. Pharmaceut. Sci., **4** (04), 652 (2015).
[10] C. Zhong, B. Qin, X. Xie, Y. Bai, J. Nano. Res-sw, **25**, 8 (2013).
[11] S – Y. Zhang, X. Chen, Y. Tian, B. K. Jin, J. X. Yang, J. Crystal Growth, **304**, 42 (2007).
[12] V. Štengl, S. Bakardjieva, J. Bludska, J. Mater. Sci., **46**, 3523 (2011).
[13] V. Nguyen, R. Amal, D. Beydoun, J. Photochem. Photobiol. A: Chemistry, **179**, 57 (2006).
[14] A. Lecomte, F. Bamiere, S. Coste, P. Thomas, J.C. Champarnaud-Mesjard, J. Europ. Cer. Soc. **27**, 1151 (2007).
[15] S. Hodgson, L. Weng, J. Non-Cryst. Sol., **276**, 195 (2000).
[16] N. Rangelova, N. Georgieva**,** K. Mileva, R.Yuryev, R. Müller, Compt. Rend. Acad. Bulg. Sci., **65** (8), 1057 (2012).
[17] V. Nu Hoai Nguyen, R. Amal, D. Beydoun, Chem. Engineer. Sci., **60**, 5759 (2005).
[18] Vi Nu Hoai Ngyen, D. Beydoun, R. Amal, J. Photochem. Photobiol. A: Chemistry, **171**, 113 (2005).
[19] Z. S. Mandough, Fizika, **2** (1), 35 (1993).
[20] G. Dai, S. Liang, H. Liu, Z. Zhong, J. Mol. Catal. A: Chemical, **368-369**, 38 (2013).
[21] Ze Da Meng, L. Zhu, K. Ullah, S. Ye, W. – Ch. Oh, Mater. Res. Bull., **56**, 45 (2014).
[22] E. M. Neville, M. J. Mattle, D. Loughrey, B. Rajesh, M. Rahman, J. M. Don MacElroy, J. A. Sullivan, K. Ravindranathan Thampi, J. Phys. Chem., C, **116**, 16511 (2012).
[23] Y. Wu, M. Xing, J. Zhang, J. Hazard. Mater., **192**, 368 (2011).
[24] N. Serpone, J. Phys. Chem. B, **110**, 24287 (2006).
[25] K. Dědkova, L. Matějova, K. Matějova, P. Peikertova, K. Mamulova Kutlakova, J. Kukutschova, Nanocon-2013, 16-18.10 Brno, Czech Republic (2013).

*Corresponding author: albenadb@svr.igic.bas.bg